ICSO 2016

International Conference on Space Optics

Biarritz, France

18–21 October 2016

Edited by Bruno Cugny, Nikos Karafolas and Zoran Sodnik

Laser ranging interferometer on Grace follow-on

C. Dahl

A. Baatzsch

M. Dehne

F. Gilles

et al.

LASER RANGING INTERFEROMETER ON GRACE FOLLOW-ON

C. Dahl[1], A. Baatzsch[1], M. Dehne[1], F. Gilles[1], P. Hager[1], M. Herding[1], K. Nicklaus[1], K. Voss[1], K. Abich[2],
C. Braxmaier[2], M. Gohlke[2], B. Guenther[2], J. Sanjuan[2], B. Zender[2], G. F. Barranco[3], A. Görth[3], C. Mahrdt[3],
V. Müller[3], D. Schütze[3], G. Stede[3], G. Heinzel[3]

[1]SpaceTech GmbH, Germany, [2]Deutsches Zentrum für Luft- und Raumfahrt e.V., Germany, [3]Albert-Einstein-Institut Hannover, Germany

I. INTRODUCTION

The Gravity Recovery and Climate Experiment (GRACE) is a successful Earth observation mission launched in 2002 consisting of two identical satellites in a polar low-Earth orbit [1]. The distance variations between these two satellites are measured with a Micro Wave Instrument (MWI) located in the central axis. In data post-processing the spatial and temporal variations of the Earth's gravitational field are recovered, which are among other things introduced by changing groundwater levels or ice-masses [2, 3, 4, 5]. The Laser Ranging Interferometer (LRI) on-board the GRACE Follow-On (GFO) mission, which will be launched in 2017 by the joint collaboration between USA (NASA) and Germany (GFZ), is a technology demonstrator to provide about two orders of magnitude higher measurement accuracy than the initial GRACE MWI, about 80 nm/√Hz in the measurement band between 2 mHz and 0.1 Hz. The integration of the LRI units on both GFO S/C has been finished in summer 2016.

The design as well as the functional, performance, and thermal-vacuum tests results of the German LRI flight units will be presented.

II. LRI OVERVIEW

The two GFO satellites, which will follow each other in a near polar orbit at 450 km height with a distance of about 220 km to each other, contain both identical LRI H/W. The LRI H/W on each S/C consists of units from the USA; these are the Laser Ranging Processor (LRP), the Laser (LAS), and the Cavity (CAV); and the main units from Germany which are the Optical Bench Subsystem [OBS, consisting of the Optical Bench Assembly (OBA) and associated Optical Bench Electronics (OBE)] and the Triple Mirror Assembly (TMA). Fig. 1 shows an overview sketch of the whole instrument configuration.

The LRI distance measurement principle is based on a laser interferometer evaluating the heterodyne signal between near-infrared single frequency lasers (λ=1064 nm) with a frequency offset in the MHz range (4 to 16 MHz). On S/C 1 (the master S/C) the laser is frequency locked to the reference CAV and the main portion of the beam is launched via a fibre injector into the OBA. Here the beam is directed and imaged onto Quadrant Photo Receivers (QPR) (which consists of two Photo Receiver Frontends (PRFs) at the OBA and one Photo Receiver Backend in the OBE) as well as to the other spacecraft via a beam splitter (BS1) and the TMA. This laser beam is called Transmitted (TX) beam and the laser beams on PRF 1 & 2 are the so-called Local Oscillator (LO). The TX beam passes the TMA, which enables the range measurement from CoM to CoM of the two spacecraft, due to its retroreflector properties and the placement of its vertex at the CoM of the respective S/C. While in principle a retroreflector is required to realize a "racetrack configuration", on GRACE FO the TMA has the further purpose to route the beam around the Ka-band horn and the coldgas tank. This requires that the TMA
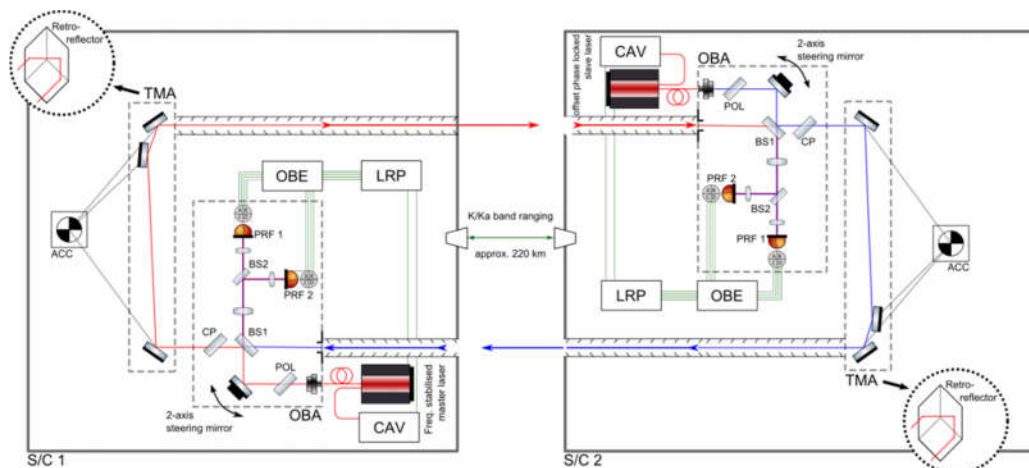

Fig. 1. Overview of the two GRACE Follow-On satellites, which shows the most important parts of the Laser Ranging Interferometer.

provides a displacement of about 600 mm between the received and transmitted beam paths. The very constrained space on the GRACE FO platforms together with the required Beam Co-Alignment (BCA) in the range of 50 µrad makes this a challenge on its own. On S/C 2 (the slave S/C) the laser is not locked to the reference cavity, but frequency offset locked to the received TX beam signal from the master S/C. Thus S/C 2 sends out a frequency shifted copy of the TX laser beam from S/C 1 back towards S/C 1. The heterodyne signal of the superposition of the LO beam on the master S/C and the received TX beam signal from the slave S/C yields two times the Doppler shift of the relative motion of the two S/C [6, 7, 8]. This heterodyne signal also contains the main science signal from which the distance variations will be derived to ultimately reconstruct the gravity field.

III. LRI-D DESIGN

This section presents the design of the German LRI flight units.

A. Optical Bench Subsystem

The OBA features an ultra-stable Fibre Injector Assembly (FIA) [10], the Fine Steering Mirror (FSM), the laser signal superposition (via beam splitter BS1), and imaging optics as well as the PRFs, which contain Quadrant Photo Diodes (QPDs). The key functions of the mentioned components are to
- Launch the laser beam to the other S/C (via the TMA)
- Direct the superimposed received TX beam and the local oscillator onto the QPD´s of the PRFs
- Convert the optical heterodyne signal to electrical signals and provide them to the LRP, which calculates the longitudinal signal as well as the angular difference between the TX beam and LO beam
- Enable the beam steering (by LRP command) to cover the field of regard of the S/C
- Enable closed-loop beam steering (by LRP) to keep the received beam and the transmitted beam co-aligned
- Image the OBA entrance aperture and the FSM optical surface onto the PRFs (for beam size adaption, avoidance of beam walk, avoidance of diffraction rings)

The key requirements for the optical bench are low optical losses, low beam distortion, low sensitivity to thermal and rotational variations as well a precision beam angle measurements and beam steering. The overall ranging noise has to be lower than 5 nm/√Hz in the thermal environment of the GFO S/C and the angular error needs to be less than a few µrad with a received signal power of some tens of pW.

Fig. 2 shows the opto-mechanical setup of the OBA. The individual components are either placed in or attached to the optical bench body which is made of titanium. This approach has been selected to achieve a low thermal noise (due to the high thermal mass enclosing the components) and high beam pointing stability (due to the symmetry of the titanium body with respect to the plane containing the beam). The optical components are made of BK7G18, which is well CTE-matched to titanium, further improving the thermal stability of the OBA.

The OBE implements the drive and control components for the FSM as well as analogue data processing capabilities for PRF signals. The key requirements of the FSM part of the OBE are to realize a small signal bandwidth of at least 1 kHz and an optical pointing noise of less than 2 µrad/√Hz. The key requirements of the QPR are to realize an equivalent input current noise of less than 5 pA/√Hz for frequencies up to 16 MHz and differential phase offsets between any 2 of the 4 AC channels of less than 100 mrad; see [6, 7, 8] for more details on the design of the OBS.
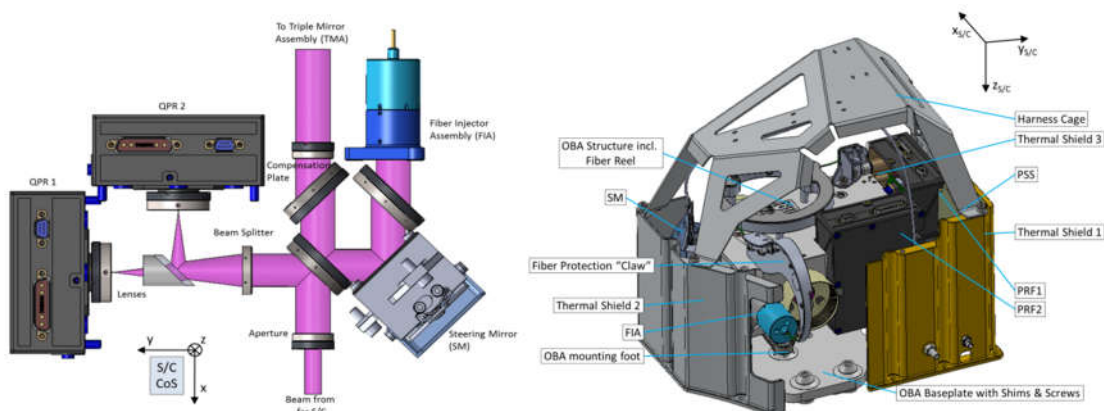

Fig. 2. Illustration of the Optical Bench Assembly. Left: top down view, showing the optical path. Right: top side view, showing the mechanical parts. The MLI, which covers the harness cage is not shown.

B. Triple Mirror Assembly

The opto-mechanical design of the TMA is depicted in Fig. 3. It consists of a mechanical frame, two mirror assemblies and a reference plate, which is required for testing purposes. The TMA mechanical frame consists of a CFRP tube and a mounting bracket interfacing with the S/C. The two mirror assemblies consist of two end fittings which are glued to the CFRP tube and three plane mirrors mounted via the glass fittings to the mechanical frame such that these three mirror planes are orthogonal to each other and intersect in the so-called vertex point. The reference plate is made of Invar, since the thermal expansion coefficient is identical to the CTE of the CFRP bracket. During all tests this plate was attached to the TMA bracket. It has been removed before integration into S/C.

One basic function of such a triple mirror, which is based on an ideal retroreflector design, is the parallelism of the reflected beam (outgoing beam on M3) and the incoming beam (incident beam on M1) while being independent of any rotation of the TMA around its vertex point. In case of any deviation of the mirror orientations from the nominal orientation to each other, the reflected beam is not perfectly parallel to the incoming beam for all angles of incidence. The BCA error (half-cone angle) of the TMA has to be small to point with the TX beam into the direction of the RX beam / other S/C. It shall be less than 40 μrad (optical) in orbit over lifetime over the field of view of the TMA.

The Optical Path Length (OPL) change with temperature between the three TMA mirrors has to be small, too, because it cannot be distinguished from an OPL change between both S/C. It shall not exceed 400 nm/K.

IV. FUNCTIONAL, PERFORMANCE AND THERMAL-VACUUM TEST RESULTS

This section presents the most important functional, performance and thermal-vacuum tests results of the German LRI flight units.

A. Test of the Optical Bench Subsystem

A schematic of OBS Thermal Vacuum (TV) test setup is shown in Fig. 4. The OBS is placed inside a large vacuum chamber onto a thermal plate. The temperature of this plate is controlled via a process thermostat in a temperature range from -30 °C to +60 °C. The LRI-D EGSE mimics the function of the LRP. It is used to control the OBS functions, read-out its monitor signals and to read-out the phase information of the OBS. The main light source of the OBA is an NPRO laser, which is connected via a fiber system to the FIA of the OBA. Using this light source the position of the LO on the QPD´s can be measured as well as the TX beam properties. The free-space TX beam of the OBA is directed through a view port out of the TV chamber to be able to measure its optical properties. Its beam angle is measured by an autocollimator (ACO), its beam diameter by a CCD camera and its wavefront by a Shack-Hartmann sensor (SHS). The ACO is also used to measure the angular alignment of a reference surface at the TX beam output of the OBA and of the reference targets in front of the OBA. Using both alignment information it is possible to derive the angular information of the TX beam w.r.t. the OBA and to suppress angular misalignments between the ACO and the OBA. A fraction of the main light source is directed via a fiber system and via a frequency shifting OGSE to the RX beam OGSE. The RX beam OGSE consists of a large fiber collimator, whose alignment can be changed in the $y_{S/C}$ and $z_{S/C}$ directions and along the rotational degree of freedom around these axes. Thus, the frequency shifted beam of the RX beam OGSE mimics the RX beam onboard of the real satellites and generates a heterodyne beat note with the LO beam inside the OBA. This is used to measure the differential wavefront sensing (DWS) coefficients of the OBA [9]. The main light source can be exchanged with an amplitude modulated laser diode to measure the differential phase offsets between the QPR channels.
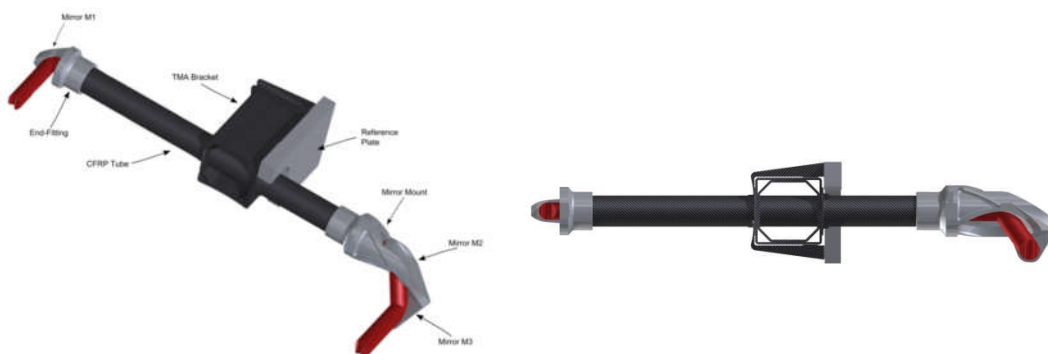

Fig. 3. Opto-mechanical design of the TMA. Left: top side view. Right: front view.
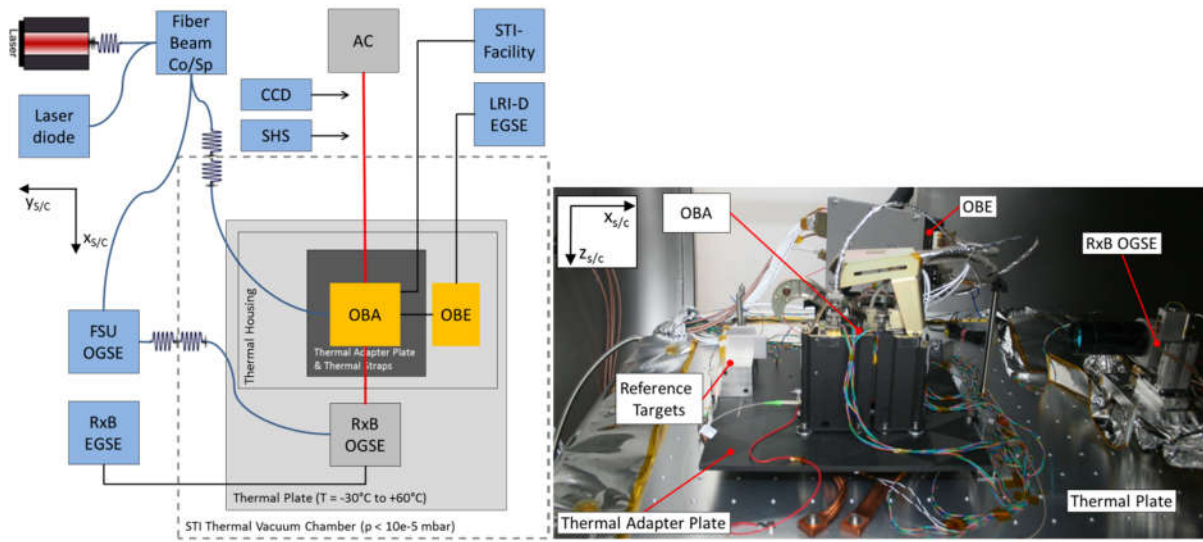
Fig. 4. Test setup of the OBS thermal vacuum test. Left: schematic. Right: photograph of the setup on the thermal plate.

For the initial acquisition of the LRI it is important to know in which direction the TX beam is pointing. Thus the change of the TX beam pointing w.r.t. the OBA is required to be smaller than 5 µrad/K. During a TV test the angular stability of the TX beam was measured at each temperature with the ACO. The rms value of this time series was calculated and corrected by the angular alignment of the reference mirrors monitored by the ACO. The measurement results are depicted in Fig. 5. A TX beam alignment change of -3.98 µrad/K in $y_{S/C}$ direction and 1.53 µrad/K in $z_{S/C}$ direction was deduced, being well within the required value of 5 µrad/K.

The wavefront error of the TX beam needs to be below λ/8 (with λ=1064 nm), which corresponds to 0.133 µm, to achieve a high heterodyne efficiency between the interfering LO and RX beams inside the OBA. At each temperature level the wavefront of the TX beam was measured over a beam diameter of 5 mm. These measurements were corrected by piston, tip and tilt wavefront errors. The results are depicted in Fig. 6. At all temperatures the corrected wavefronts and Zernike wavefronts of the TX beam fulfil the requirement
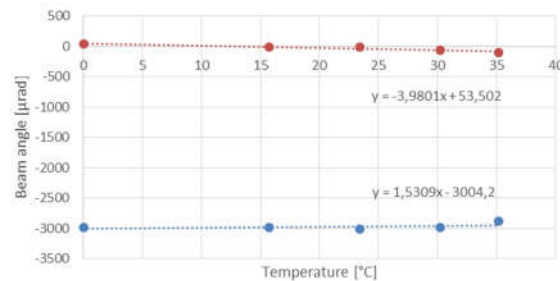

Fig. 5. TX beam angle at OBA output over temperature. The red dots correspond to $y_{S/C}$ and the blue to $z_{S/C}$.
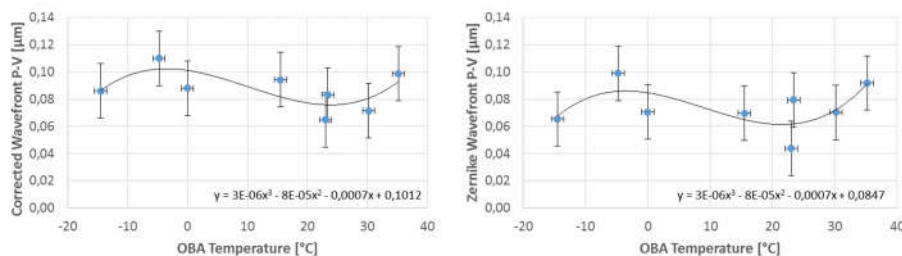

Fig. 6. TX beam wavefront error over temperature. Left: corrected wavefront peak-valley. Right: Zernike wavefront peak-valley. The solid line represents the polynomial fit to the measurement value. y is the fitted function.
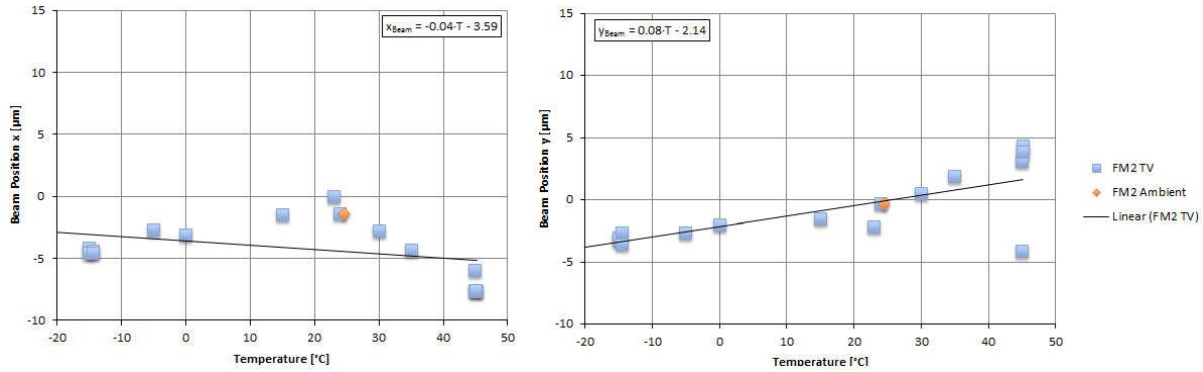
Fig. 7. Local Oscillator beam position on the quadrant photodiode on PRF 1 as a function of temperature. Left: alignment along x-axis; right: alignment along y-axis.

The beam position of the LO beam on the PRFs is a good measure for the differential stability of the OBA optics and it was required that LO beam is centered on the PRF better than 10 µm. The beam position of the LO on the PRF1 as a function of temperature is depicted in Fig. 7. This requirement is fulfilled over the complete temperature range. The beam position of the LO on PRF2 shows a similar behavior and fulfils the requirement, too.

The phase of the science signal will be provided to the LRP via the 4 AC channels of the QPR. The LRP will process the phase and will generate the average of all four phase signals as well as the DWS combinations of the four phase signals. The latter one is used to control the optical pointing of the TX beam via the FSM. Thus the differential phase error between the 4 AC channels of the QPR will have a similar influence on the TX beam pointing like the BCA error of the TMA; see Subsection III. B. Therefore the differential phase stability between any 2 of the 4 AC channels of the QPR needs to be below 15 mrad/K in the frequency range of the science signal, which is 4 to 16 MHz. This property of the QPR was measured and the left graph in Fig. 8 depicts the maximum value of the temperature coefficients of the differential phase, while both PRF were operated. The graphs of the other PRF combinations have a similar slope. The temperature coefficient for the differential phase offset (for the complete QPR chain) is far below 1 mrad/K. Hence, the requirement is fulfilled. The average phase contains the information about the distance variation between both S/C. Therefore the average phase stability of the 4 AC channels of the QPR will have a similar influence on the ranging signal like the OPL stability of the TMA; see Subsection III. B. The average phase stability of the four AC channels of the QPR has to be better than 50 mrad/K between 4 and 16 MHz. The right graph in Fig. 8 depicts the maximum value of the temperature coefficients of the average phase stability. The average phase stability is better than -5 mrad/K.
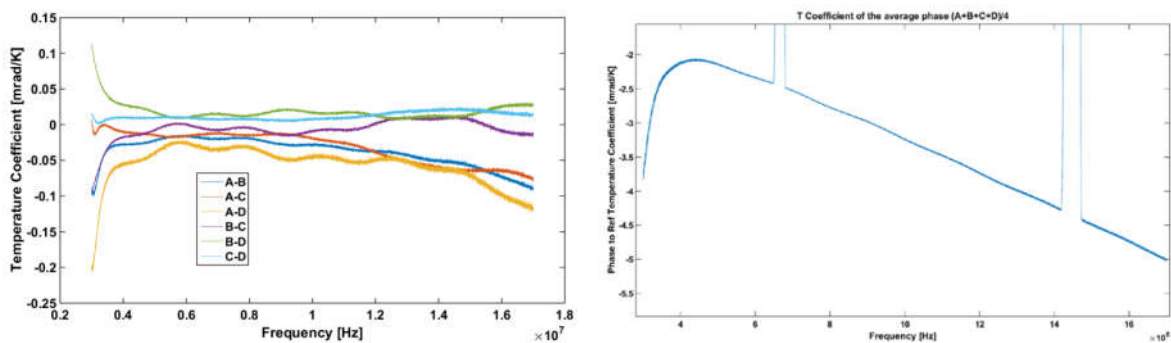

Fig. 8. Left: temperature coefficient of the phase difference of all QPR channels combinations, while both PRFs are operating. Right: temperature coefficient of the average phase of all QPR channels, while both PRFs are operating. The two peaks visible in the plot are an artifact produced by the down sampling of the data combinations with phase wrapping of the measured signals.

B. Test of the Triple Mirror Assembly

The BCA error of the TMA was measured at room temperature for horizontal and vertical (g-compensated) orientations of the TMA as well as in a thermal vacuum environment for horizontal orientations of the TMA. In Fig. 9 the test setup for the measurement of the BCA error of the TMA over temperature is shown. The ACO and a beam multiplexing system are located outside of a TV chamber. The TMA and the reference flat are installed on a CFRP plate inside the TV chamber. The reference flat is made of Zerodur[TM] and has two reflecting surfaces, which are parallel on the µrad level to each other. The reference flat enables the angular measurement of a test beam before and after it passes twice the TMA. The angular misalignment between the direct reflection from the reference flat and the indirect reflection via the TMA yields the information about the BCA error of the TMA.

The TMA and the reference flat are mounted on an ultra-stable CFRP baseplate. Different temperature levels have to be maintained for these two items. Therefore, they are mounted inside separate thermal enclosures compartments. The reference flat is kept always at room temperature to minimize angular misalignments of its reflecting surfaces. The TMA temperature is changed over the operational flight temperature range to measure the temperature coefficient of the BCA error. The reference flat is mounted inside the OGSE thermal box. The TMA is located inside the TMA thermal enclosure. Both compartments are thermally controlled by heaters and temperature sensors in a closed-loop control. The BCA of the TMA is measured using the autocollimator.

Within the TMA FM1 BCA test campaign the linear thermal coefficients were determined to be 2.43 µrad/K for rotation around y and 2.44 µrad/K for rotation around z in a temperature range of -5 °C ≤ T ≤ 30 °C.

After the BCA TV test campaign the BCA measurement in vertical (g-compensated) orientation of the TMA at room temperature was performed. The final co-alignment values were -8.39 µrad for rotation around the z-axis and -11.97 µrad for rotation around the y-axis. The measured difference between the horizontal BCA during TV test and the vertical BCA is 1.12 µrad for rotation around z and 2.28 µrad for rotation around y. It has been shown that this behaviour is reversible.

Fig. 9 shows the BCA dependence over temperature including error analysis and the 40 µrad top level requirement. For this assessment the error of the temperature measurement was assumed to be 1.1 K (rms) and the error of the tilt measurement was assumed to be 5.4 µrad (rms). The BCA half-cone angle is 48.9 µrad at 10 °C and 20.21 µrad at 30 °C.

The OPL temperature coefficient of the TMA was measured in a thermal vacuum environment for horizontal orientation of the TMA. The test setup is shown in Fig. 10 .The laser head, the phasemeter and the two Differential Plane Mirror Interferometer (DPMI) from Zygo are located outside of the TV chamber. These parts are mounted on a stable table and additional optics including polarising optics are needed to route the light through the setup via a view port to the setup inside the TV chamber. The Zygo DPMIs are rotated by 45° w.r.t. to each other in order to be able to reach the corner cube behind the TMA (beams have to be routed around the TMA tube and through the TMA bracket). Polarising optics, half- and quarter-wave plates, are necessary for cleaning up the polarization and to avoid polarization mixing errors, thus, minimizing the parasitic beat note. The TMA, its reference plate and a corner cube are mounted via an adapter plate to an ultra-stable CFRP plate inside the TV chamber. The corner cube vertex coincides with the TMA vertex and thus the corner cube is used to reference the OPL change to the TMA vertex position. The interferometer mirrors (which are: reference mirrors with holes M1 and R1 and plane target mirrors M2 and R2) are installed on a separate CFRP plate and located in a thermally stabilized environment to achieve the required measurement accuracy of better than 200 nm/K.
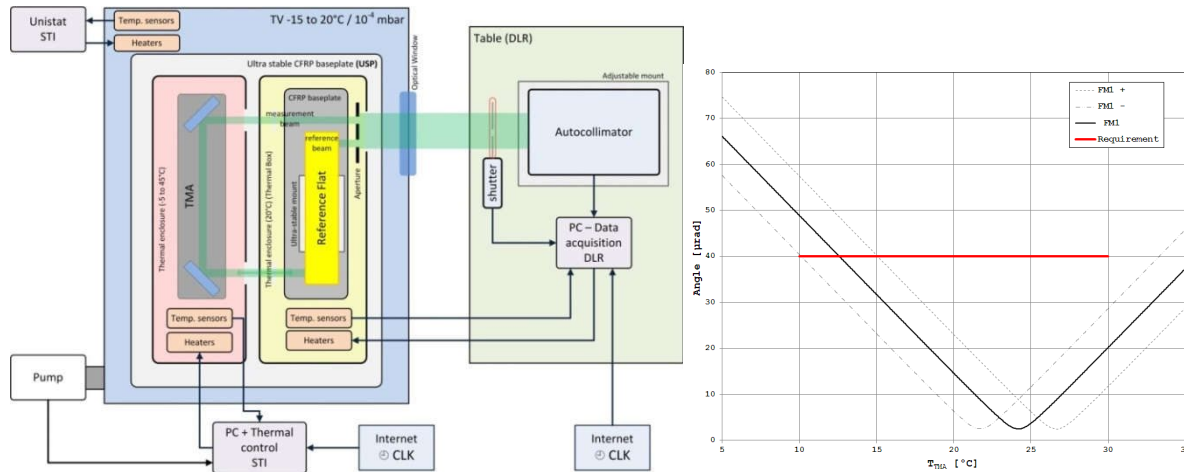
Fig. 9. Left: Test setup for the measurement of the beam co-alignment error of the TMA over temperature. Right: The determined temperature dependence of the rotational angles is applied on the measured angles of the g-compensated TMA FM1 including an error assessment. The extrapolation is based on a co-alignment of -11.97 µrad (rotation around y) and -8.39 µrad (rotation around z) at 20 °C. Red: 40 µrad requirement.
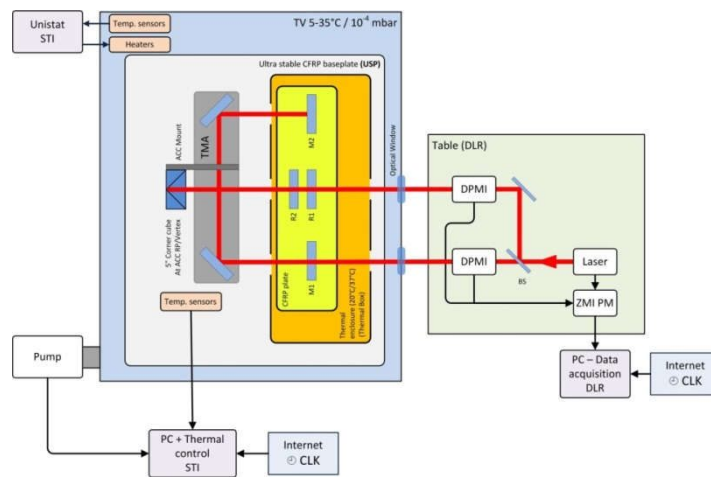

Fig. 10. Test setup for the measurement of the optical path length error of the TMA.

The OPL coefficient has been processed for different temperature ranges. The resulting coefficients are 563 nm/K ± 111 nm/K for temperatures between -5 °C and +45 °C and 515 nm ± 40 nm/K for temperatures between +5 °C and +35 °C. Although the OPL coefficient is slightly above the requirement of 400 nm/K the measured OPL coefficient will not limit the measurement performance of the GRACE FO satellites because the temperature stability, which has been assumed for the requirement of 400 nm/K at the beginning, is much better on the S/C.

VI. SUMMARY

We have presented the design of the German units of the laser ranging interferometer on GRACE FO and the test results of the key electro-optical requirements achieved with the flight models. It was verified that the flight models will enable the LRI to establish an optical link between the two GRACE FO satellites and to perform ranging measurements with the required precision. The LRI is expected to demonstrate a significantly reduced ranging noise compared to the MWI and to enable even higher accuracy measurements of Earth's gravity field.

The delivery of the German LRI units to the S/C has started in spring 2016. The German LRI units have been successfully integrated on both S/C. The environmental tests on S/C level will start in autumn 2016.

ACKNOWLEDGEMENT

REFERENCES

[1] http://www.gfz-potsdam.de/grace
[2] I. Sasgen, M. van den Broeke, J. L. Bamber, E. Rignot, L. S. Sørensen, B. Wouters, Z. Martinec, I. Velicogna, S. B. Simonsen, "Timing and origin of recent regional ice-mass loss in Greenland," *Earth and Planetary Science Letters*, vol. 333-334, pp. 293-303, 2012.
[3] V. M. Tiwari, J. Wahr, S. Swenson, "Dwindling groundwater resources in northern India, from satellite gravity observations," *Geophys. Research Lett.,* vol 36, pp. L18401, 2009.
[4] J. S. Famiglietti, ,M. Lo, S. L. Ho, J. Bethune, K. J. Anderson, T. H. Syed, S. C. Swenson, C. R. de Linage, M. Rodell, "Satellites measure recent rates of groundwater depletion in California's Central Valley," *Geophys. Research Lett.*, vol. 38, pp. L03403, 2011.
[5] J. T. Reager, B. F. Thomas, and J. S. Famiglietti, "River basin flood potential inferred using GRACE gravity observations at several months lead time," *Nature Geoscience.* vol. 7, pp. 588-592, 2014.
[6] G. Heinzel, B. Sheard, N. Brause, K. Danzmann, M. Dehne, O. Gerberding, C. Mahrdt, V. Mueller, D. Schuetze, G. Stede, W. Klipstein, W. Folkner, R. Spero, K. Nicklaus, P. Gath, D. Shaddock, "Laser Ranging Interferometer for GRACE follow-on," *International Conference on Space Optics*, 2012.
[7] B. S. Sheard, G. Heinzel, K. Danzmann, D. A. Shaddock, W.M. Klipstein, W. M. Folkner, "Intersatellite laser ranging instrument for the GRACE follow-on mission," *Journal of Geodesy*, vol. 86, pp. 1083-1095, 2012.
[8] K. Nicklaus, M. Herding, A. Baatzsch, M. Dehne, C. Diekmann, K. Voss, F. Gilles. B. Guenther, B. Zender, S. Boehme, V. Mueller, D. Schuetze, G. Stede, B. Sheard, G. Heinzel, "Optical Bench of the Laser Ranging Interferometer on GRACE Follow-On," *International Conference on Space Optics,* 2014.
[9] G. Hechenblaikner, "Measurement of the absolute wavefront curvature radius in a heterodyne interferometer,". *Journal of the Optical Society of America*, 27, 2010.
[10] S. Boehme, S. Fabian, A. Kamm, T. Beschel, E. Beckert, A. Tünnermann, K. Nicklaus, M. Dehne, "High Reproducible CO2 Laser Spliced Fiber-Collimator for a Space Borne Laser System," *International Conference on Space Optics,* 2016.